Life Sciences 113 (2014) 45–54

Contents lists available at ScienceDirect

Life Sciences

journal homepage: www.elsevier.com/locate/lifescie

Genome-wide analysis of DNA methylation in UVB- and DMBA/TPA-induced mouse skin cancer models

Anne Yuqing Yang [a,b,c,1], Jong Hun Lee [a,b,h,1], Limin Shu [a,b], Chengyue Zhang [a,b,c], Zheng-Yuan Su [a,b], Yaoping Lu [a,d], Mou-Tuan Huang [a,d], Christina Ramirez [b,e], Douglas Pung [b], Ying Huang [a,b,c], Michael Verzi [f], Ronald P. Hart [g], Ah-Ng Tony Kong [a,b,d,*]

[a] Center for Cancer Prevention Research, Ernest Mario School of Pharmacy, Piscataway, NJ 08854, USA
[b] Department of Pharmaceutics, Ernest Mario School of Pharmacy, Piscataway, NJ 08854, USA
[c] Graduate Program in Pharmaceutical Sciences, Ernest Mario School of Pharmacy, Piscataway, NJ 08854, USA
[d] Susan Lehman Cullman Laboratory for Cancer Research, Department of Chemical Biology, Ernest Mario School of Pharmacy, Piscataway, NJ 08854, USA
[e] Graduate Program in Cellular and Molecular Pharmacology, Rutgers, The State University of New Jersey, Piscataway, NJ 08854, USA
[f] Department of Genetics, Rutgers, The State University of New Jersey, Piscataway, NJ 08854, USA
[g] Department of Cell Biology and Neuroscience, Rutgers, The State University of New Jersey, Piscataway, NJ 08854, USA
[h] Department of Food Science and Biotechnology, CHA university, Kyunggi, Korea

ARTICLE INFO

Article history:
Received 6 May 2014
Accepted 21 July 2014
Available online 2 August 2014

Keywords:
DNA methylation
Epigenetics
MeDIP-Seq
UVB
DMBA/TPA

ABSTRACT

Aims: Ultraviolet irradiation and carcinogens have been reported to induce epigenetic alterations, which potentially contribute to the development of skin cancer. We aimed to study the genome-wide DNA methylation profiles of skin cancers induced by ultraviolet B (UVB) irradiation and 7,12-dimethylbenz(a)anthracene (DMBA)/12-O-tetradecanoylphorbol-1,3-acetate (TPA).

Main methods: Methylated DNA immunoprecipitation (MeDIP) followed by next-generation sequencing was utilized to ascertain the DNA methylation profiles in the following common mouse skin cancer models: SKH-1 mice treated with UVB irradiation and CD-1 mice treated with DMBA/TPA. Ingenuity® Pathway Analysis (IPA) software was utilized to analyze the data and to identify gene interactions among the different pathways.

Key findings: 6003 genes in the UVB group and 5424 genes in the DMBA/TPA group exhibited a greater than 2-fold change in CpG methylation as mapped by the IPA software. The top canonical pathways identified by IPA after the two treatments were ranked were pathways related to cancer development, cAMP-mediated signaling, G protein-coupled receptor signaling and PTEN signaling associated with UVB treatment, whereas protein kinase A signaling and xenobiotic metabolism signaling were associated with DMBA/TPA treatment. In addition, the mapped IL-6-related inflammatory pathways displayed alterations in the methylation profiles of inflammation-related genes linked to UVB treatment.

Significance: Genes with altered methylation were ranked in the UVB and DMBA/TPA models, and the molecular interaction networks of those genes were identified by the IPA software. The genome-wide DNA methylation profiles of skin cancers induced by UV irradiation or by DMBA/TPA will be useful for future studies on epigenetic gene regulation in skin carcinogenesis.

Introduction

Accumulating evidence suggests that epigenetic DNA alterations play a crucial role in cancer initiation and development. Specifically, aberrant DNA methylation at the 5′-position of cytosine in CG dinucleotides in the cancer genome is postulated to be the most relevant epigenetic change in cancer (Esteller, 2008). DNA methylation affects gene expression and therefore regulates a wide range of biological processes, including proliferation, cell death, mutation and cancer initiation/promotion/progression (Momparler and Bovenzi, 2000; Zingg and Jones, 1997). Both global hypomethylation and regional hypermethylation are characteristics of tumorigenesis (Baylin et al., 2000; Laird and Jaenisch, 1996). DNA hypermethylation at promoter regions is a predominant epigenetic mechanism for reducing the expression of tumor suppressor genes. Epigenetic silencing of tumor suppressor genes has been reported in mouse models of malignant tumors (Chen et al., 2003; Tommasi et al., 2005). Thus, the present study aimed to profile

Abbreviations: MeDIP, methylated DNA immunoprecipitation; UV, ultraviolet; UVA, ultraviolet A; UVB, ultraviolet B; DMBA, 7,12-dimethylbenz(a)anthracene; TPA, 12-O-tetradecanoylphorbol-1,3-acetate; IPA, Ingenuity® Pathway Analysis; IL, interleukin.

* Corresponding author at: Rutgers, The State University of New Jersey, Ernest Mario School of Pharmacy, Room 228, 160 Frelinghuysen Road, Piscataway, NJ 08854, USA. Tel.: +1 848 445 6369/8; fax: +1 732 445 3134.
E-mail address: kongt@pharmacy.rutgers.edu (A.-N.T. Kong).

[1] These authors contributed equally to this work.

http://dx.doi.org/10.1016/j.lfs.2014.07.031
0024-3205/

the global DNA methylation changes that occur during carcinogenesis. To address this aim, we conducted global profiling of DNA methylation changes in two representative skin carcinogenesis models, ultraviolet B (UVB)-exposed SKH-1 hairless mice and DMBA/TPA-induced carcinogenesis in CD-1 mice.

Ultraviolet irradiation has been reported to induce epigenetic alterations, which may contribute to the development of skin cancer (Nandakumar et al., 2011). However, the precise mechanism by which UV irradiation is related to carcinogenesis remains unclear. In addition, a method for screening epigenetically modified genes in melanoma patients needs to be established (Koga et al., 2009; Kanavy and Gerstenblith, 2011). Mutations in oncogenes and tumor suppressor genes have been reported in melanoma. However, most of these mutations are not present in non-melanoma skin cancer (Hocker and Tsao, 2007), suggesting a specific role for UV irradiation in carcinogenesis. In skin tumors, UV irradiation has been reported to induce epigenetic modifications and may contribute to the development of skin cancer. Epigenetic changes, such as DNA methylation and histone modification, may play a crucial role in the initiation and development of certain types of cancer (Ballestar and Esteller, 2008). Epigenetic alterations generally represent the interface between the environment and the genome (Jaenisch and Bird, 2003).

The multistage skin carcinogenesis model is established by applying a sub-threshold dose of the carcinogen DMBA followed by repetitive treatments with the tumor promoter TPA. With three well-defined stages—initiation, promotion, and progression—this model is similar to natural human tumor development. This model has been widely used to investigate the anti-tumor efficacy of chemicals and the molecular events that occur during each stage of tumor development. Several genetic alterations identified in human skin cancer patients have also been described in the mouse multistage skin carcinogenesis model, such as changes in cyclin D1 (Wilkey et al., 2009), TP53 (Saab et al., 2009), CDKN21 (Nishijo et al., 2009) and PTEN (Zheng et al., 2008). The underlying similarity in the biology of cancer between mice and humans implies that genes related to mouse tumor development may also be relevant to human tumor development.

In the present study, we used methylated DNA immunoprecipitation (MeDIP) coupled with next-generation sequencing to profile the whole genome DNA methylation patterns from the UVB and DMBA/TPA models. The MeDIP-Seq results were evaluated by Ingenuity® Pathway Analysis (IPA) to investigate genetic crosstalk and signal/function overlap. The present study included an initial assessment of genes with a modified methylation profile and the identification of interacting molecular networks in skin carcinogenesis models.

Materials and methods

Chemicals and antibodies

The chemicals used in the current study were as follows: 7,12-dimethylbenz(a)anthracene (DMBA; Sigma-Aldrich, MO, USA) and 12-O-tetradecanoylphorbol-1,3-acetate (TPA; Alexis Co., CA, USA). The 5-methylcytidine monoclonal antibody was purchased from Eurogentec., Belgium.

Mice and skin cancer induction

Two representative skin carcinogenesis models were utilized in the present study. SKH-1 hairless female mice, 7–8 weeks old, were treated with UVB (30 mJ/cm^2) twice a week for 36 weeks. The ultraviolet (UV) lamps (FS72T12-UVB-HO; National Biological, Twinsburg, OH) emitted UVB (280–320 nm; 70–80% of the total energy) and ultraviolet A (UVA) (320–375 nm; 20–75% of the total energy). The dose of UVB was quantified using a UVB Spectra 305 dosimeter (The Daavlin Company, Bryan, OH). The radiation was further calibrated using a research radiometer/photometer (model IL-1700; International Light Inc., Newburyport, MA). The mice were assessed twice weekly for the appearance of papillomas and carcinomas. Skin papilloma and carcinoma samples were collected, frozen in liquid nitrogen and stored at −80 °C. The epidermises of age-matched untreated mice were isolated from fresh skin as a control group.

Six-week-old female CD-1 mice were used for the DMBA/TPA-induced multistage carcinogenesis model. One day before treatment, the backs of the mice were shaved. For tumor initiation, 200 nmol DMBA in 200 μL of acetone was applied on the back skin of the mice. Three days after DMBA treatment, 5 nmol TPA in 200 μL of acetone was applied three times a week for 11 weeks to induce tumor promotion and progression.

Global analysis of methylated DNA

Genomic DNA (gDNA) was extracted from UV irradiation-induced tumor samples from 3 female mice and from non-irradiated epidermis samples from 3 female age-matched SKH-1 mice; from female CD-1 mice in the DMBA/TPA-induced carcinogenesis model for the MeDIP-Seq assay. gDNA was extracted using a DNeasy Kit (Qiagen, Valencia, CA) according to the manufacturer's protocol. The gDNA was electrophoresed on an agarose gel, and the OD ratios were determined to confirm the purity and concentration of the gDNA prior to fragmentation by Covaris (Covaris, Inc., Woburn, MA USA). Fragmented gDNA was evaluated for size distribution and concentration using an Agilent Bioanalyzer 2100 and a NanoDrop spectrophotometer.

MeDIP-Seq

MeDIP was performed to analyze genome-wide methylation. MeDIP was performed using a MagMeDIP Kit from Diagenode according to the manufacturer's instructions. Methylated DNA was recovered by immunoprecipitation with antibodies specific to methylated cytosine used to separate methylated DNA fragments from unmethylated fragments, and Illumina libraries were created from the captured gDNA using NEBNext reagents (catalog# E6040; New England Biolabs, Ipswich, MA, USA). Enriched libraries were evaluated for size distribution and concentration using an Agilent Bioanalyzer 2100. The samples were then sequenced on an Illumina HiSeq2000 machine, which generated paired-end reads of 90 or 100 nucleotides (nt). The results were analyzed for data quality and exome coverage using the platform provided by DNAnexus (DNAnexus, Inc., Mountain View, CA, USA). Samples were sent to Otogenetics Corporation (Norcross, GA) for Illumina sequencing and alignment with the genome. The resulting BAM files were downloaded for analysis.

MeDIP alignments were compared with control samples using Cuffdiff 2.0.2 with no length correction (Trapnell et al., 2012). Briefly,

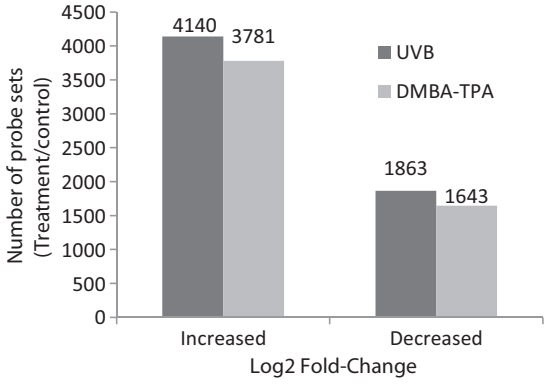

Fig. 1. Total number of significantly increased and decreased genes based on changes in methylation (≥2-fold change in Log_2) in the UVB and DMBA/TPA groups.

Table 1
Top 50 annotated genes with increased methylation ranked by log_2 fold change. (A) UVB group. (B) DMBA/TPA group.

(A)

Rank	Symbol	Gene name	Log_2 fold change (UVB/control)	Location	Type(s)
1	RBFOX1	RNA binding protein, fox-1 homolog (*C. elegans*) 1	5.457	Cytoplasm	Other
2	IMPG2	Interphotoreceptor matrix proteoglycan 2	5.367	Extracellular space	Other
3	DGKK	Diacylglycerol kinase, kappa	5.31	Cytoplasm	Kinase
4	MAD1L1	MAD1 mitotic arrest deficient-like 1 (yeast)	5.252	Nucleus	Other
5	EVX2	Even-skipped homeobox 2	5.19	Nucleus	Transcription regulator
6	PAN3	PAN3 poly(A) specific ribonuclease subunit homolog (*S. cerevisiae*)	4.989	Cytoplasm	Other
7	AAMP	Angio-associated, migratory cell protein	4.837	Plasma membrane	Other
8	ARHGAP18	Rho GTPase activating protein 18	4.837	Cytoplasm	Other
9	ACAA2	Acetyl-CoA acyltransferase 2	4.574	Cytoplasm	Enzyme
10	OLFM1	Olfactomedin 1	4.574	Cytoplasm	Other
11	TGS1	Trimethylguanosine synthase 1	4.574	Nucleus	Enzyme
12	DYM	Dymeclin	4.525	Cytoplasm	Other
13	Hspg2	Heparan sulfate proteoglycan 2	4.474	Extracellular space	Other
14	Kcnip2	Kv channel-interacting protein 2	4.474	Plasma membrane	other
15	TNS1	Tensin 1	4.474	Plasma membrane	Other
16	AGAP1	ArfGAP with GTPase domain, ankyrin repeat and PH domain 1	4.367	Cytoplasm	Enzyme
17	CCDC180	Coiled–coil domain containing 180	4.367	Other	Other
18	EDN1	Endothelin 1	4.367	Extracellular space	Cytokine
19	FOXE1	Forkhead box E1 (thyroid transcription factor 2)	4.367	Nucleus	Transcription regulator
20	KCNN4	Potassium intermediate/small conductance calcium-activated channel, subfamily N, member 4	4.367	Plasma membrane	Ion channel
21	LOXHD1	Lipoxygenase homology domains 1	4.367	Extracellular space	Other
22	DCP2	Decapping mRNA 2	4.252	Nucleus	Enzyme
23	DET1	De-etiolated homolog 1 (Arabidopsis)	4.252	Nucleus	Other
24	DSC3	Desmocollin 3	4.252	Plasma membrane	Other
25	HOXD11	Homeobox D11	4.252	Nucleus	Transcription regulator
26	MAML2	Mastermind-like 2 (Drosophila)	4.252	Nucleus	Transcription regulator
27	MYO1E	Myosin IE	4.252	Cytoplasm	Enzyme
28	PCBD1	Pterin-4 alpha-carbinolamine dehydratase/dimerization cofactor of hepatocyte nuclear factor 1 alpha	4.252	Nucleus	Transcription regulator
29	WNT3	Wingless-type MMTV integration site family, member 3	4.252	Extracellular space	Other
30	CENPF	Centromere protein F, 350/400 kDa	4.126	Nucleus	Other
31	Dos	Downstream of Stk11	4.126	Other	Other
32	FBXO11	F-box protein 11	4.126	Cytoplasm	Enzyme
33	GPR37	G protein-coupled receptor 37 (endothelin receptor type B-like)	4.126	Plasma membrane	G-protein coupled receptor
34	HPCA	Hippocalcin	4.126	Cytoplasm	Other
35	LIMS2	LIM and senescent cell antigen-like domains 2	4.126	Cytoplasm	Other
36	LRRC8B	Leucine rich repeat containing 8 family, member B	4.126	Other	Other
37	LTA4H	Leukotriene A4 hydrolase	4.126	Cytoplasm	Enzyme
38	MEMO1	Mediator of cell motility 1	4.126	Cytoplasm	Other
39	mir-221	MicroRNA 221	4.126	Cytoplasm	MicroRNA
40	mir-802	MicroRNA 802	4.126	Cytoplasm	MicroRNA
41	Olfr1323	Olfactory receptor 1323	4.126	Plasma membrane	G-protein coupled receptor
42	PLN	Phospholamban	4.126	Cytoplasm	Transporter
43	PTPN23	Protein tyrosine phosphatase, non-receptor type 23	4.126	Cytoplasm	Phosphatase
44	SLC7A9	Solute carrier family 7 (amino acid transporter light chain, bo, + system), member 9	4.126	Plasma membrane	Transporter
45	VRK1	Vaccinia related kinase 1	4.126	Nucleus	Kinase
46	ZBTB34	Zinc finger and BTB domain containing 34	4.126	Nucleus	Other
47	ZNF622	Zinc finger protein 622	4.126	Nucleus	Other
48	SMYD2	SET and MYND domain containing 2	4.082	Cytoplasm	Enzyme
49	DYSF	Dysferlin, limb girdle muscular dystrophy 2B (autosomal recessive)	3.989	Plasma membrane	Other
50	Ear2 (includes others)	Eosinophil-associated, ribonuclease A family, member 2	3.989	Cytoplasm	Enzyme

(B)

Rank	Symbol	Gene name	Log_2 fold change (DMBA-TPA/control)	Location	Type(s)
1	FAM135A	Family with sequence similarity 135, member A	5.974	Other	Enzyme
2	CADM2	Cell adhesion molecule 2	5.231	Plasma membrane	Other
3	VWC2L	von Willebrand factor C domain containing protein 2-like	4.877	Extracellular space	Other
4	PTH2R	Parathyroid hormone 2 receptor	4.708	Plasma membrane	G-protein coupled receptor
5	NPY	Neuropeptide Y	4.515	Extracellular space	Other
6	TNS1	Tensin 1	4.408	Plasma membrane	Other

(*continued on next page*)

Table 1 *(continued)*

(B)

Rank	Symbol	Gene name	Log_2 fold change (DMBA-TPA/control)	Location	Type(s)
7	PHYHIPL	Phytanoyl-CoA 2-hydroxylase interacting protein-like	4.408	Cytoplasm	Other
8	COX7C	Cytochrome c oxidase subunit VIIc	4.408	Cytoplasm	Enzyme
9	CMYA5	Cardiomyopathy associated 5	4.408	Plasma membrane	Other
10	HELB	Helicase (DNA) B	4.351	Nucleus	Enzyme
11	WDR63	WD repeat domain 63	4.292	Other	Other
12	SIPA1L2	Signal-induced proliferation-associated 1 like 2	4.292	Other	Other
13	let-7	MicroRNA let-7a-1	4.292	Cytoplasm	MicroRNA
14	DSEL	Dermatan sulfate epimerase-like	4.292	Extracellular space	Enzyme
15	ZNF521	Zinc finger protein 521	4.167	Nucleus	Other
16	TMTC2	Transmembrane and tetratricopeptide repeat containing 2	4.167	Cytoplasm	Other
17	OTOL1	Otolin 1	4.167	Other	Other
18	METTL21A	Methyltransferase like 21A	4.167	Other	Enzyme
19	INTU	Inturned planar cell polarity protein	4.167	Cytoplasm	Other
20	DHCR7	7-dehydrocholesterol reductase	4.167	Cytoplasm	Enzyme
21	Cyp2a12/Cyp2a22	Cytochrome P450, family 2, subfamily a, polypeptide 12	4.167	Cytoplasm	Enzyme
22	CTSC	Cathepsin C	4.167	Cytoplasm	Peptidase
23	CHORDC1	Cysteine and histidine-rich domain (CHORD) containing 1	4.167	Other	Other
24	CBLN1	Cerebellin 1 precursor	4.167	Cytoplasm	Other
25	THAP1	THAP domain containing, apoptosis associated protein 1	4.029	Nucleus	Other
26	RYBP	RING1 and YY1 binding protein	4.029	Nucleus	Transcription regulator
27	NDUFA12	NADH dehydrogenase (ubiquinone) 1 alpha subcomplex, 12	4.029	Cytoplasm	Enzyme
28	Mug1/Mug2	Murinoglobulin 1	4.029	Extracellular space	Transporter
29	MFSD10	Major facilitator superfamily domain containing 10	4.029	Other	Transporter
30	KIF16B	Kinesin family member 16B	4.029	Cytoplasm	Enzyme
31	GRID2	Glutamate receptor, ionotropic, delta 2	4.029	Plasma membrane	Ion channel
32	Gm4836 (includes others)	Predicted gene 4836	4.029	Cytoplasm	Other
33	FOXN3	Forkhead box N3	4.029	Nucleus	Transcription regulator
34	Cyp4f16/Gm9705	Cytochrome P450, family 4, subfamily f, polypeptide 16	4.029	Cytoplasm	Enzyme
35	CXorf22	Chromosome X open reading frame 22	4.029	Other	Other
36	Pag1	phosphoprotein associated with glycosphingolipid microdomains 1	3.955	Plasma membrane	other
37	MSH6	MutS homolog 6	3.923	Nucleus	Enzyme
38	ZFAT	Zinc finger and AT hook domain containing	3.877	Nucleus	Other
39	Vmn1r188 (includes others)	Vomeronasal 1 receptor 217	3.877	Plasma membrane	G-protein coupled receptor
40	TYW3	tRNA-yW synthesizing protein 3 homolog (*S. cerevisiae*)	3.877	Other	Other
41	TPO	Thyroid peroxidase	3.877	Plasma membrane	Enzyme
42	TLR4	Toll-like receptor 4	3.877	Plasma membrane	Transmembrane receptor
43	THSD7B	Thrombospondin, type I, domain containing 7B	3.877	Other	Other
44	SPINK5	Serine peptidase inhibitor, Kazal type 5	3.877	Extracellular space	Other
45	SLC9A8	Solute carrier family 9, subfamily A (NHE8, cation proton antiporter 8), member 8	3.877	Cytoplasm	Transporter
46	SEC23A	Sec23 homolog A (*S. cerevisiae*)	3.877	Cytoplasm	Transporter
47	RPS4Y1	Ribosomal protein S4, Y-linked 1	3.877	Cytoplasm	Other
48	PPP1R1C	Protein phosphatase 1, regulatory (inhibitor) subunit 1C	3.877	Cytoplasm	Phosphatase
49	PARP8	Poly(ADP-ribose) polymerase family, member 8	3.877	Other	Other
50	NLRP4	NLR family, pyrin domain containing 4	3.877	Cytoplasm	Other

a list of overlapping regions of sequence alignment common to both the immunoprecipitated and the control samples was created and used to judge the quantitative enrichment in MeDIP samples over control samples using Cuffdiff; statistically significant peaks at 5% FDR and a minimum 4-fold difference using the Cummerbund package in R were selected (Trapnell et al., 2012). Peaks were matched with adjacent annotated genes using ChIPpeakAnno (Zhu et al., 2010).

Functional and pathway analysis by Ingenuity® Pathway Analysis (IPA)

We analyzed lists of genes with significant fold changes (based on the *P* values; UV-induced tumor vs. control and DMBA/TPA treatment vs. control) in the methylation pattern (increases and decreases) ascertained in the MeDIP-Seq experiment using Ingenuity® Pathways Analysis 4.0 (IPA 4.0, Ingenuity Systems, www.ingenuity.com). IPA utilized gene symbols that were identified as neighboring enriched methylation peaks by ChIPpeakAnno used for all of the analyses. IPA mapped 6003 genes in the UVB group and 5424 genes in the DMBA/TPA group with a ≥2-fold change compared with the control correspondingly. Based on these fold change data, IPA identified biological functions and canonical pathways related to UVB-induced cancer. The list of genes within canonical pathways was ranked using the ratio of the number of genes mapped to each pathway to the total number of genes in the corresponding pathway, which is presented as observations/total in Table 3.

Table 2
Top 50 annotated genes with decreased methylation ranked by log_2 fold change. (A) UVB group. (B) DMBA/TPA group.

(A)

	Symbol	Gene name	Log_2 fold change (UVB/control)	Location	Type(s)
1	Nrxn3	Neurexin III	−4.543	Plasma membrane	Other
2	SYN2	Synapsin II	−4.378	Plasma membrane	Other
3	Mup1 (includes others)	Major urinary protein 1	−4.333	Extracellular space	Other
4	KRT86	Keratin 86	−4.24	Cytoplasm	Other
5	SULT1C3	Sulfotransferase family, cytosolic, 1C, member 3	−4.24	Cytoplasm	Enzyme
6	ATP1A3	ATPase, Na+/K+transporting, alpha 3 polypeptide	−4.191	Plasma membrane	Transporter
7	CHORDC1	Cysteine and histidine-rich domain (CHORD) containing 1	−4.191	Other	Other
8	NRXN1	Neurexin 1	−4.191	Plasma membrane	Transporter
9	Htr6	5-Hydroxytryptamine (serotonin) receptor 6, G protein-coupled	−4.141	Plasma membrane	G-protein coupled receptor
10	PAM	Peptidylglycine alpha-amidating monooxygenase	−4.141	Plasma membrane	Enzyme
11	SERPINB3	Serpin peptidase inhibitor, clade B (ovalbumin), member 3	−4.141	Cytoplasm	Other
12	TDRD3	Tudor domain containing 3	−4.141	Nucleus	Transcription regulator
13	Olfr1153	Olfactory receptor 1153	−4.088	Plasma membrane	G-protein coupled receptor
14	WFIKKN2	WAP, follistatin/kazal, immunoglobulin, kunitz and netrin domain containing 2	−4.088	Other	Other
15	ABAT	4-Aminobutyrate aminotransferase	−4.034	Cytoplasm	Enzyme
16	ARHGAP6	Rho GTPase activating protein 6	−4.034	Cytoplasm	other
17	AUH	AU RNA binding protein/enoyl-CoA hydratase	−4.034	Cytoplasm	Enzyme
18	CEP70	Centrosomal protein 70 kDa	−4.034	Cytoplasm	Other
19	DGKH	Diacylglycerol kinase, eta	−4.034	Cytoplasm	Kinase
20	GRIA1	Glutamate receptor, ionotropic, AMPA 1	−4.034	Plasma membrane	Ion channel
21	SLC4A7	Solute carrier family 4, sodium bicarbonate cotransporter, member 7	−4.034	Plasma membrane	Transporter
22	SLITRK1	SLIT and NTRK-like family, member 1	−4.034	Other	Other
23	Speer4a (includes others)	Spermatogenesis associated glutamate (E)-rich protein 4a	−4.034	Nucleus	Other
24	CETN1	Centrin, EF-hand protein, 1	−3.977	Nucleus	Enzyme
25	CYLC1	Cylicin, basic protein of sperm head cytoskeleton 1	−3.977	Cytoplasm	Other
26	HS3ST5	Heparan sulfate (glucosamine) 3-O-sulfotransferase 5	−3.977	Cytoplasm	Enzyme
27	Ott (includes others)	Ovary testis transcribed	−3.977	Other	Other
28	Scg5	Secretogranin V	−3.977	Cytoplasm	Other
29	CHM	Choroideremia (Rab escort protein 1)	−3.918	Cytoplasm	Enzyme
30	Clvs2	Clavesin 2	−3.918	Cytoplasm	Other
31	MRPS30	Mitochondrial ribosomal protein S30	−3.918	Cytoplasm	Enzyme
32	Olfr1010	Olfactory receptor 1010	−3.918	Plasma membrane	G-protein coupled receptor
33	PPP1R12A	Protein phosphatase 1, regulatory subunit 12A	−3.918	Cytoplasm	Phosphatase
34	ZMYND11	Zinc finger, MYND-type containing 11	−3.918	Nucleus	Other
35	ADCY10	Adenylate cyclase 10 (soluble)	−3.857	Cytoplasm	Enzyme
36	Agtr1b	Angiotensin II receptor, type 1b	−3.857	Plasma membrane	G-protein coupled receptor
37	APAF1	Apoptotic peptidase activating factor 1	−3.857	Cytoplasm	Other
38	AQP1	Aquaporin 1	−3.857	Plasma membrane	Transporter
39	CDH10	Cadherin 10, type 2 (T2-cadherin)	−3.857	Plasma membrane	Other
40	CHRM3	Cholinergic receptor, muscarinic 3	−3.857	Plasma membrane	G-protein coupled receptor
41	GCNT2	Glucosaminyl (N-acetyl) transferase 2, I-branching enzyme (I blood group)	−3.857	Cytoplasm	Enzyme
42	GNAI1	Guanine nucleotide binding protein (G protein), alpha inhibiting activity polypeptide 1	−3.857	Plasma membrane	Enzyme
43	SELENBP1	Selenium binding protein 1	−3.857	Cytoplasm	Other
44	SP110	SP110 nuclear body protein	−3.857	Nucleus	Other
45	TMEM5	Transmembrane protein 5	−3.857	Plasma membrane	Other
46	XIRP2	Xin actin-binding repeat containing 2	−3.857	Other	Other
47	ZKSCAN2	Zinc finger with KRAB and SCAN domains 2	−3.857	Nucleus	Transcription regulator
48	1700009N14Rik	RIKEN cDNA 1700009N14 gene	−3.793	Other	Transporter
49	AGPAT9	1-Acylglycerol-3-phosphate O-acyltransferase 9	−3.793	Cytoplasm	Enzyme
50	ASCL1	Achaete–scute complex homolog 1 (Drosophila)	−3.793	Nucleus	Transcription regulator

(B)

Rank	Symbol	Gene name	Log_2 fold change (DMBA-TPA/control)	Location	Type(s)
1	EBPL	Emopamil binding protein-like	−5.292	Cytoplasm	Enzyme
2	PANX1	Pannexin 1	−5.247	Plasma membrane	Transporter
3	HES5	Hairy and enhancer of split 5 (Drosophila)	−4.632	Nucleus	Other
4	LHX4	LIM homeobox 4	−4.247	Nucleus	Transcription regulator
5	GSG1L	GSG1-like	−4.247	Plasma membrane	Other
6	PBX1	Pre-B-cell leukemia homeobox 1	−4.199	Nucleus	Transcription regulator
7	LRRC8B	Leucine rich repeat containing 8 family, member B	-4.199	Other	Other
8	ASAH2		−4.199	Cytoplasm	Enzyme

(continued on next page)

Table 2 *(continued)*

(B)					
	Symbol	Gene name	Log_2 fold change (DMBA-TPA/control)	Location	Type(s)
		N-acylsphingosine amidohydrolase (non-lysosomal ceramidase) 2			
9	ALKBH3	alkB, alkylation repair homolog 3 (E. coli)	−4.199	Nucleus	Enzyme
10	ZNF518B	Zinc finger protein 518B	−4.100	Other	Other
11	MAN1A1	Mannosidase, alpha, class 1A, member 1	−4.100	Cytoplasm	Enzyme
12	TOX3	TOX high mobility group box family member 3	−3.993	Other	Other
13	LSM11	LSM11, U7 small nuclear RNA associated	−3.936	Nucleus	Other
14	TCEA3	Transcription elongation factor A (SII), 3	−3.877	Nucleus	Transcription regulator
15	OR7D2	Olfactory receptor, family 7, subfamily D, member 2	−3.877	Plasma membrane	G-protein coupled receptor
16	KIAA0947	KIAA0947	−3.877	Other	Other
17	CBLB	Cbl proto-oncogene B, E3 ubiquitin protein ligase	−3.877	Nucleus	Other
18	NOS1AP	Nitric oxide synthase 1 (neuronal) adaptor protein	−3.816	Cytoplasm	Other
19	MACC1	Metastasis associated in colon cancer 1	−3.816	Nucleus	Other
20	ZNF277	Zinc finger protein 277	−3.752	Nucleus	Transcription regulator
21	Sp100	Nuclear antigen Sp100	−3.752	Nucleus	Transcription regulator
22	KCNA6	Potassium voltage-gated channel, shaker-related subfamily, member 6	−3.752	Plasma membrane	Ion channel
23	C19orf10	Chromosome 19 open reading frame 10	−3.752	Extracellular space	Cytokine
24	TMEM17	Transmembrane protein 17	−3.685	Extracellular space	Other
25	FAM92B	Family with sequence similarity 92, member B	−3.650	other	Other
26	TBC1D5	TBC1 domain family, member 5	−3.646	Extracellular space	Other
27	Nrg1	Neuregulin 1	−3.614	Extracellular space	Growth factor
28	GORASP1	Golgi reassembly stacking protein 1, 65 kDa	−3.614	Cytoplasm	Other
29	AHRR	Aryl-hydrocarbon receptor repressor	−3.614	Nucleus	Other
30	ADORA2A	Adenosine A2a receptor	−3.614	Plasma membrane	G-protein coupled receptor
31	RAB11A	RAB11A, member RAS oncogene family	−3.540	Cytoplasm	Enzyme
32	ISY1-RAB43	ISY1-RAB43 readthrough	−3.540	Nucleus	Other
33	GNE	Glucosamine (UDP-N-acetyl)-2-epimerase/N-acetylmannosamine kinase	−3.540	Cytoplasm	Kinase
34	FAM98A	Family with sequence similarity 98, member A	−3.540	Other	Other
35	ENPP4	Ectonucleotide pyrophosphatase/phosphodiesterase 4 (putative)	−3.540	Other	Enzyme
36	CCDC43	Coiled–coil domain containing 43	−3.540	Other	Other
37	ARHGEF10	Rho guanine nucleotide exchange factor (GEF) 10	−3.540	Cytoplasm	Enzyme
38	TARSL2	Threonyl-tRNA synthetase-like 2	−3.462	Other	Enzyme
39	SCARB1	Scavenger receptor class B, member 1	−3.462	Plasma membrane	Transporter
40	RAB27A	RAB27A, member RAS oncogene family	−3.462	Cytoplasm	Enzyme
41	L3MBTL3	l(3)mbt-like 3 (Drosophila)	−3.462	Nucleus	Other
42	Higd1a	HIG1 domain family, member 1A	−3.462	Cytoplasm	Other
43	GRIA1	Glutamate receptor, ionotropic, AMPA 1	−3.462	Plasma membrane	Ion channel
44	GPC5	Glypican 5	−3.462	Plasma membrane	Other
45	CLGN	Calmegin	−3.462	Cytoplasm	Peptidase
46	CHKA	Choline kinase alpha	−3.462	Cytoplasm	Kinase
47	ASGR1	Asialoglycoprotein receptor 1	−3.462	Plasma membrane	Transmembrane receptor
48	AMY2A	Amylase, alpha 2A (pancreatic)	−3.462	Extracellular space	Enzyme
49	C1orf109	Chromosome 1 open reading frame 109	−3.444	Other	Other
50	CADPS	Ca++-dependent secretion activator	−3.430	Plasma membrane	Other

Results

MeDIP-Seq results

Skin samples were collected from the UVB- and DMBA/TPA-induced mouse skin cancer models, and gDNA was isolated from each sample. A whole-genome DNA methylation analysis was performed on the DNA samples using the described MeDIP-Seq method. The results were analyzed in a paired manner comparing the tumor to the normal skin tissue samples for each model.

In the UVB group, 6003 genes were identified in the two samples with a≥2-fold change in methylation. Compared with the control, 4140 genes exhibited increased methylation, and methylation was decreased in 1863 genes (Fig. 1). However, in the DMBA/TPA treatment group, 5424 genes were identified with a≥2-fold change in peak reads between the tumor and the normal skin samples. Among these 5424 genes, the methylation pattern was increased in 3781 genes and decreased in 1643 genes. To prioritize those changes, we ranked the top 50 increased (+, Table 1) and decreased (−, Table 2) genes based on the log_2 fold change from highest to lowest, all with *P* values less than 0.05.

Table 3
Top 5 altered canonical pathways determined using Ingenuity Pathways Software in the UVB and DMBA/TPA groups. The shared pathways are shown in bold.

Rank	Name	Ratio	Observation/total	p-Value
UVB/control				
1	cAMP-mediated signaling	0.478	108/226	1.27E−09
2	G-protein coupled receptor signaling	0.442	122/276	5.24E−09
3	**Molecular mechanisms of cancer**	**0.371**	**144/388**	**9.86E−07**
4	PTEN signaling	0.42	58/138	5.21E−06
5	Role of osteoblasts, osteoclasts and chondrocytes in rheumatoid arthritis	0.388	97/250	5.58E−06
DMBA–TPA/control				
1	Protein kinase A signaling	0.352	144/409	5.5E−06
2	**Molecular mechanisms of cancer**	**0.325**	**126/338**	**4.57E−05**
3	Xenobiotic metabolism signaling	0.351	101/288	7.59E−05
4	Regulation of the epithelial–mesenchymal transition pathway	0.342	67/196	0.0011
5	Mouse embryonic stem cell pluripotency	0.394	39/99	0.0013

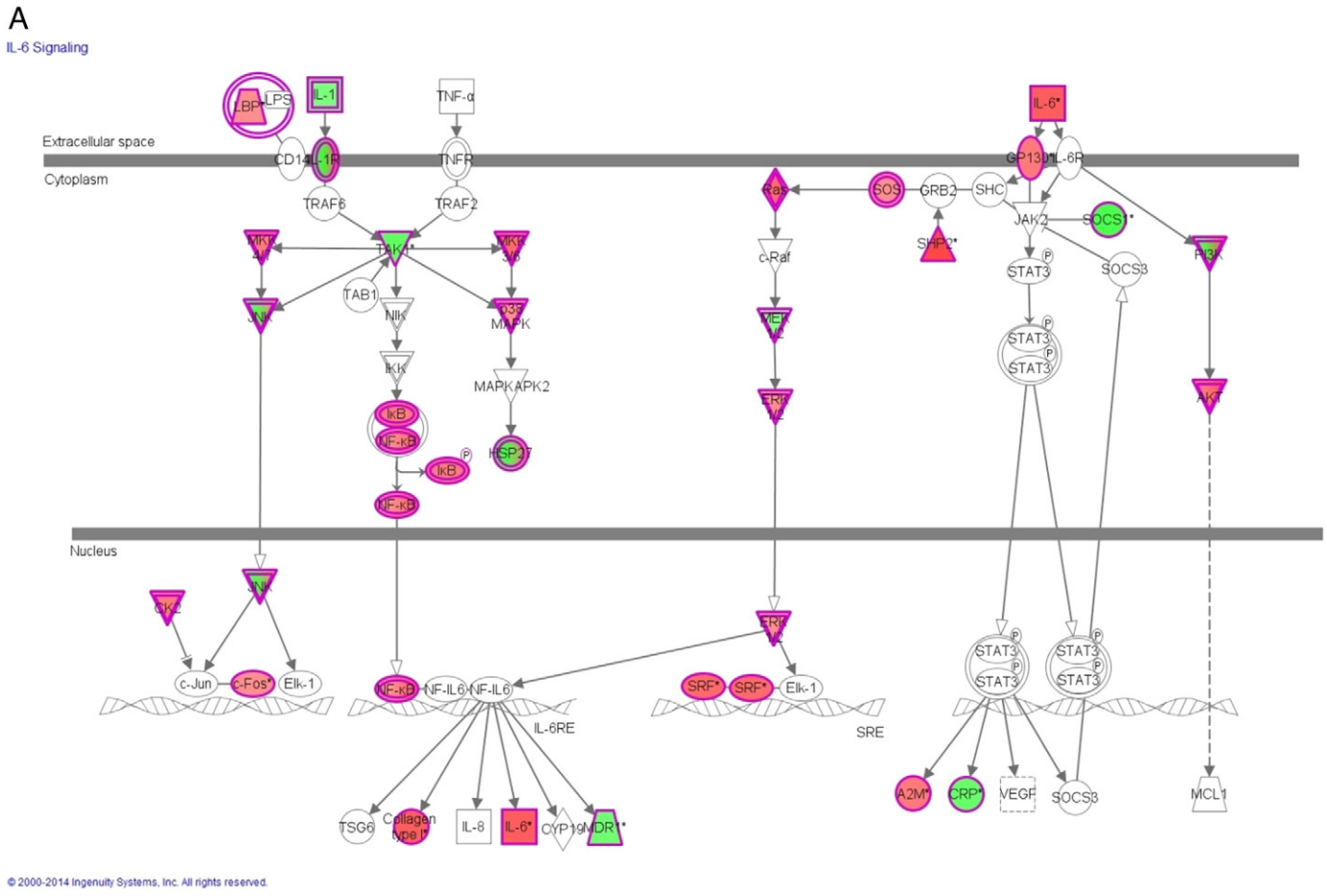

Fig. 2. (A) Genes mapped to the IL-6 pathway by IPA software. Red, increased methylation; green, decreased methylation; UVB irradiated vs. control. (B) List of genes mapped to the IL-6 pathway by IPA.

Pathway analysis by IPA

To ascertain the significance of the methylation changes, 6003 genes in the UVB group and 5424 genes in the DMBA/TPA group with a greater than 2-fold change in methylation were analyzed using the Ingenuity® Pathway Analysis (IPA) software package. The top 5 canonical signaling pathways were categorized (Table 3) based on the ratio of the number of input genes to the total number of genes in the corresponding pathway in the Ingenuity® Pathway Analysis software. Fisher's exact test was used to calculate *P* values to determine the significance of the associations of the input genes with the canonical pathways.

IPA identified more than 50 signaling pathways containing genes with significantly increased and decreased methylation. The interleukin-6 (IL-6)-related signaling pathway was mapped by IPA to the UVB group (Fig. 2); the methylation profile is presented in red (increase) and green (decrease). Fig. 2B lists the genes involved in the IL-6 signaling pathway that exhibited altered methylation (14 increased and 30 decreased) as mapped by IPA. It has been reported that IL-6 protein expression is induced by UV irradiation (Vaid et al., 2010). Correspondingly, the MeDIP-Seq data revealed that *IL-6* increased methylation by 3.252-fold ($\log_2$). Based on the IPA functional pathways, skin cancer belongs to the category of mechanism of cancer. The top 5 genes related to skin cancer based on IPA are ranked by fold change in Table 4. This list includes genes with increased methylation and genes with decreased methylation that are related to skin cancer pathways by IPA.

Discussion

It was previously reported that hypermethylation of CpG islands in tumor suppressor genes occurs in human squamous cell carcinoma cell lines and in primary skin tumor tissues. Similar changes in DNA methylation patterns were observed in the multistage mouse skin cancer model. In addition, loss of global genomic methylation has been shown to be associated with increased aggressiveness of mouse skin cancer cell lines. However, the precise mechanism by which UV irradiation promotes melanoma remains unclear. Furthermore, there is no method for screening potential epigenetically modified genes involved in promoting skin cancers (Kanavy and Gerstenblith, 2011; Jhappan et al., 2003; Leiter and Garbe, 2008; Moan et al., 2008). Long-term exposure to UV irradiation is considered a major etiologic risk factor for the development of melanoma and non-melanoma skin cancers. Epigenetic alterations are generally considered to represent the interface between the environment and the genome (Jaenisch and Bird, 2003). Ultraviolet irradiation has been reported to induce epigenetic alterations, which may contribute to the development of skin cancer. In the present study, we performed global genome methylation screening using MeDIP-Seq to identify genomic loci with aberrant methylation patterns in cancer tissues.

One of the adverse effects of UV irradiation that has been observed in skin tumor development is a chronic and sustained inflammatory response. The relationship between inflammation and epigenetic modifications in cancer is under active investigation (Nile et al., 2008; Tekpli et al., 2013; Gasche et al., 2011). In this

B

	Log_2 Fold Change (UVB/Control)	Symbol	Gene Name
Decreased			
1	-3.421	*IL1RAPL2*	interleukin 1 receptor accessory protein-like 2
2	-3.24	*HSPB3*	heat shock 27kDa protein 3
3	-3.141	*MAPK10*	mitogen-activated protein kinase 10
4	-3.141	*PIK3C2G*	phosphatidylinositol-4-phosphate 3-kinase, catalytic subunit type 2 gamma
5	-3.141	*SOCS1*	suppressor of cytokine signaling 1
6	-2.918	*PIK3R1*	phosphoinositide-3-kinase, regulatory subunit 1 (alpha)
7	-2.793	*IL1RL1*	interleukin 1 receptor-like 1
8	-2.793	*MAP3K7*	mitogen-activated protein kinase kinase kinase 7
9	-2.655	*CRP*	C-reactive protein, pentraxin-related
10	-2.503	*ABCB1*	ATP-binding cassette, sub-family B (MDR/TAP), member 1
11	-2.503	*IL1R2*	interleukin 1 receptor, type II
12	-2.333	*IL36B*	interleukin 36, beta
13	-2.141	*MAP2K1*	mitogen-activated protein kinase kinase 1
14	-2.034	*PIK3R4*	phosphoinositide-3-kinase, regulatory subunit 4
Increased			
1	3.667	*AKT3*	v-akt murine thymoma viral oncogene homolog 3
2	3.667	*PIK3CG*	phosphatidylinositol-4,5-bisphosphate 3-kinase, catalytic subunit gamma
3	3.667	*PTPN11*	protein tyrosine phosphatase, non-receptor type 11
4	3.474	*PIK3C3*	phosphatidylinositol 3-kinase, catalytic subunit type 3
5	3.252	*COL1A1*	collagen, type I, alpha 1
6	3.252	*IL6*	interleukin 6 (interferon, beta 2)
7	3.252	*RELA*	v-rel avian reticuloendotheliosis viral oncogene homolog A
8	3.169	*IL1RL2*	interleukin 1 receptor-like 2
9	2.989	*IL1RAP*	interleukin 1 receptor accessory protein
10	2.989	*MAP2K6*	mitogen-activated protein kinase kinase 6
11	2.989	*RRAS2*	related RAS viral (r-ras) oncogene homolog 2
12	2.989	*SRF*	serum response factor (c-fos serum response element-binding transcription factor)
13	2.915	*NFKB2*	nuclear factor of kappa light polypeptide gene enhancer in B-cells 2 (p49/p100)
14	2.667	*A2M*	alpha-2-macroglobulin
15	2.667	*AKT1*	v-akt murine thymoma viral oncogene homolog 1
16	2.667	*CSNK2A1*	casein kinase 2, alpha 1 polypeptide
17	2.667	*HSPB1*	heat shock 27kDa protein 1
18	2.667	*IL6ST*	interleukin 6 signal transducer (gp130, oncostatin M receptor)
19	2.667	*MAP2K4*	mitogen-activated protein kinase kinase 4
20	2.667	*NFKBIA*	nuclear factor of kappa light polypeptide gene enhancer in B-cells inhibitor, alpha
21	2.474	*PIK3C2A*	phosphatidylinositol-4-phosphate 3-kinase, catalytic subunit type 2 alpha
22	2.252	*FOS*	FBJ murine osteosarcoma viral oncogene homolog
23	2.252	*IL1R1*	interleukin 1 receptor, type I
24	2.252	*LBP*	lipopolysaccharide binding protein
25	2.252	*MAPK1*	mitogen-activated protein kinase 1
26	2.252	*MAPK8*	mitogen-activated protein kinase 8
27	2.252	*MAPK13*	mitogen-activated protein kinase 13
28	2.252	*NFKB1*	nuclear factor of kappa light polypeptide gene enhancer in B-cells 1
29	2.252	*SOS1*	son of sevenless homolog 1
30	2.252	*SOS2*	son of sevenless homolog 2

Fig. 2 (*continued*).

study, a UV irradiation-induced abnormal inflammatory response was suggested based on the IPA mapped IL-6 pathways, which included the methylation profiles of pro-inflammatory cytokines, receptors and mitogen-activated protein kinases. Higher levels of pro-inflammatory cytokines are associated with tumor development and progression (Mukhtar and Elmets, 1996; Tron et al.,

Table 4
Top 5 genes with altered methylation (increased or decreased) that were related to skin cancer using the IPA Software Functional and Diseases analysis module in the UVB and the DMBA/TPA groups. The shared genes are shown in bold.

Rank	Mapped genes	Log_2 fold change
UVB/control		
Increased		
1	RBFOX1	5.457
2	LOXHD1	4.367
3	EDN1	4.367
4	DYSF	3.989
5	NPSR1	3.837
Decreased		
1	SULT1C3	−4.24
2	ABAT	−4.034
3	**GRIA1**	**−4.034**
4	PCSK1	−3.726
5	SCN2A	−3.655
DMBA–TPA/control		
Increased		
1	GRID2	4.029
2	NLRP4	3.877
3	EMR1	3.877
4	IL15	3.877
5	PCDH18	3.708
Decreased		
1	**GRIA1**	**−3.462**
2	CADPS	−3.43
3	BCL2L11	−3.292
4	ACVR1C	−3.292
5	GRM3	−3.292

1988). Interleukins (ILs) have different systemic functions and are involved in inflammation. Nile et al. reported that the methylation of CpGs in the promoter region of *IL-6* affected the mRNA levels in mononuclear cells (Nile et al., 2008). Tekpli et al. reported that the methylation of CpGs near the *IL-6* transcriptional start site is significantly higher in non-small cell lung cancer cells and is associated with lower IL-6 mRNA expression (Tekpli et al., 2013). Our study demonstrated that *IL-6* gene methylation was significantly higher in UV irradiation-induced skin tumors.

IL-6-Jak-Stat3 inflammatory signaling is also involved in cell survival and provides a proliferative advantage in the two-stage chemical carcinogenesis model using DMBA as the tumor initiator and TPA as the promoter. Phosphorylated-Stat3 overexpression in a papilloma cell line leads to enhanced cell migration and invasion (Suiqing et al., 2005). Transgenic mice with constitutive Stat3 expression have a shorter latency period and increased tumor incidence compared with non-transgenic littermates after DMBA/TPA treatment (Chan et al., 2008). Moreover, mice with constitutively activated Stat3 bypassed the premalignant stage and were initially diagnosed with carcinoma in situ, which rapidly progressed to squamous cell carcinoma. In our present study, we found 34 genes with altered DNA methylation in total 124 genes involved in the IL-6 pathway in the UV group. Among these genes with altered methylation, the SOCS1 (suppressor of cytokine signaling 1) gene, which encodes a suppressor in the IL-6-Jak-Stat3 loop, was hypermethylated in the tumor samples.

The top-ranked hypermethylated and hypomethylated genes could enable the discovery of key genes in skin cancer development. For example, *RBFOX1* is the top increased gene in terms of methylation status change in UV-irradiated tumors compared with normal epidermis by IPA (Fig. 1). RBFOX1 is an RNA-binding protein that is highly expressed in the cytoplasm. RBFOX1 mutations were identified in colorectal cancer cell lines (CRC), and RBFOX1 deletion was observed in a significant proportion of CRC cases (106/419) (Cancer Genome Atlas, N., 2012; Sengupta et al., 2013). However, the role of RBFOX1 in skin cancer development is unclear. Surprisingly, tumor tissues from the DMBA/TPA group exhibited a unique profile in terms of the top 50 genes with increased or decreased methylation compared with the profile in the UVB group. Cell adhesion molecule 2 (*CADM2*) was one of the top methylated genes in DMBA/TPA tumors. CADM2 belongs to a protein family that participates in maintaining cell polarity and that has been considered to be a novel category of tumor suppressors (Chang et al., 2010). Clinically, low CADM2 expression predicts a high risk of recurrence in patients with hepatocellular carcinoma after hepatectomy (Yang et al., 2014). It has also been reported that aberrant promoter hypermethylation and loss of CADM2 expression are associated with human renal cell carcinoma progression (He et al., 2013). Our study is the first report to suggest that *CADM2* methylation could be involved in skin carcinogenesis. Moreover, we identified changes in the methylation patterns of several genes encoding microRNAs, which are also involved in epigenetic regulation. This observation indicates that epigenetic changes may occur at multiple levels with complex crosstalk in skin cancer development and progression.

The genes identified in this study demonstrated significant alterations in response to UV irradiation-induced inflammation and skin cancer development. Although IPA revealed some overlapping signaling changes in response to both UV irradiation and DMBA–TPA treatment and certain highly affected targets were common (including, GRIA1 and TNS1), the top-ranked genes based on fold change differed markedly between the two treatments, indicating that distinct epigenetic mechanisms trigger tumorigenesis after exposure to UV or the DMBA carcinogen.

Conclusions

In this study, a comprehensive analysis of the DNA methylation patterns in the UVB or DMBA/TPA induced tumors compared with age-matched normal skin was completed. Genes coding for inflammatory cytokines were identified by IPA to exhibit altered methylation profiles and may be associated with increased susceptibility to tumor development. Specifically, based on changes in methylation, molecular networks were identified that included genes encoding inflammatory cytokines. Additional studies with a particular emphasis on epigenetic alterations, such as DNA methylation, may lead to the development of new strategies for the prevention of skin cancer and inflammation-related skin disease.

Conflict of interest statement

The authors declare that there are no conflicts of interest.

Acknowledgments

The authors would like to thank the members of Tony Kong's laboratory for their helpful discussions. This work was supported in part by institutional funds.

References

Ballestar E, Esteller M. Epigenetic gene regulation in cancer. Adv Genet 2008;61:247–67.
Baylin SB, Belinsky SA, Herman JG. Aberrant methylation of gene promoters in cancer—concepts, misconcepts, and promise. J Natl Cancer Inst 2000;92(18):1460–1.
Cancer Genome Atlas, N. Comprehensive molecular characterization of human colon and rectal cancer. Nature 2012;487(7407):330–7.
Chan KS, Sano S, Kataoka K, Abel E, Carbajal S, Beltran L, et al. Forced expression of a constitutively active form of Stat3 in mouse epidermis enhances malignant progression of skin tumors induced by two-stage carcinogenesis. Oncogene 2008;27(8):1087–94.
Chang G, Xu S, Dhir R, Chandran U, O'Keefe DS, Greenberg NM, et al. Hypoexpression and epigenetic regulation of candidate tumor suppressor gene CADM-2 in human prostate cancer. Clin Cancer Res 2010;16(22):5390–401.
Chen WY, Zeng X, Carter MG, Morrell CN, Chiu Yen RW, Esteller, et al. Heterozygous disruption of Hic1 predisposes mice to a gender-dependent spectrum of malignant tumors. Nat Genet 2003;33(2):197–202.
Esteller M. Epigenetics in cancer. N Engl J Med 2008;358(11):1148–59.
Gasche JA, Hoffmann J, Boland CR, Goel A. Interleukin-6 promotes tumorigenesis by altering DNA methylation in oral cancer cells. Int J Cancer 2011;129(5):1053–63.

He W, Li X, Xu S, Ai J, Gong Y, Gregg JL, et al. Aberrant methylation and loss of CADM2 tumor suppressor expression is associated with human renal cell carcinoma tumor progression. Biochem Biophys Res Commun 2013;435(4):526–32.
Hocker T, Tsao H. Ultraviolet radiation and melanoma: a systematic review and analysis of reported sequence variants. Hum Mutat 2007;28(6):578–88.
Jaenisch R, Bird A. Epigenetic regulation of gene expression: how the genome integrates intrinsic and environmental signals. Nat Genet 2003;33:245–54. (Suppl.).
Jhappan C, Noonan FP, Merlino G. Ultraviolet radiation and cutaneous malignant melanoma. Oncogene 2003;22(20):3099–112.
Kanavy HE, Gerstenblith MR. Ultraviolet radiation and melanoma. Semin Cutan Med Surg 2011;30(4):222–8.
Koga Y, Pelizzola M, Cheng E, Krauthammer M, Sznol M, Ariyan S, et al. Genome-wide screen of promoter methylation identifies novel markers in melanoma. Genome Res 2009;19(8):1462–70.
Laird PW, Jaenisch R. The role of DNA methylation in cancer genetic and epigenetics. Annu Rev Genet 1996;30:441–64.
Leiter U, Garbe C. Epidemiology of melanoma and nonmelanoma skin cancer—the role of sunlight. Adv Exp Med Biol 2008;624:89–103.
Moan J, Porojnicu AC, Dahlback A. Ultraviolet radiation and malignant melanoma. Adv Exp Med Biol 2008;624:104–16.
Momparler RL, Bovenzi V. DNA methylation and cancer. J Cell Physiol 2000;183(2):145–54.
Mukhtar H, Elmets CA. Photocarcinogenesis: mechanisms, models and human health implications. Photochem Photobiol 1996;63(4):356–7.
Nandakumar V, Vaid M, Tollefsbol TO, Katiyar SK. Aberrant DNA hypermethylation patterns lead to transcriptional silencing of tumor suppressor genes in UVB-exposed skin and UVB-induced skin tumors of mice. Carcinogenesis 2011;32(4):597–604.
Nile CJ, Read RC, Akil M, Duff GW, Wilson AG. Methylation status of a single CpG site in the IL6 promoter is related to IL6 messenger RNA levels and rheumatoid arthritis. Arthritis Rheum 2008;58(9):2686–93.
Nishijo K, Chen QR, Zhang L, McCleish AT, Rodriguez A, Cho MJ, et al. Credentialing a preclinical mouse model of alveolar rhabdomyosarcoma. Cancer Res 2009;69(7):2902–11.
Saab R, Rodriguez-Galindo C, Matmati K, Rehg JE, Baumer SH, Khoury JD, et al. p18Ink4c and p53 Act as tumor suppressors in cyclin D1-driven primitive neuroectodermal tumor. Cancer Res 2009;69(2):440–8.
Sengupta N, Yau C, Sakthianandeswaren A, Mouradov D, Gibbs P, Suraweera N, et al. Analysis of colorectal cancers in British Bangladeshi identifies early onset, frequent mucinous histotype and a high prevalence of RBFOX1 deletion. Mol Cancer 2013;12:1.
Suiqing C, Min Z, Lirong C. Overexpression of phosphorylated-STAT3 correlated with the invasion and metastasis of cutaneous squamous cell carcinoma. J Dermatol 2005;32(5):354–60.
Tekpli X, Landvik NE, Anmarkud KH, Skaug V, Haugen A, Zienolddiny S. DNA methylation at promoter regions of interleukin 1B, interleukin 6, and interleukin 8 in non-small cell lung cancer. Cancer Immunol Immunother 2013;62(2):337–45.
Tommasi S, Dammann R, Zhang Z, Wang Y, Liu L, Tsark WM, et al. Tumor susceptibility of Rassf1a knockout mice. Cancer Res 2005;65(1):92–8.
Trapnell C, Roberts A, Goff A, Pertea G, Kim D, Kelley DR, et al. Differential gene and transcript expression analysis of RNA-seq experiments with TopHat and Cufflinks. Nat Protoc 2012;7(3):562–78.
Tron VA, Rosenthal D, Sauder DN. Epidermal interleukin-1 is increased in cutaneous T-cell lymphoma. J Invest Dermatol 1988;90(3):378–81.
Vaid M, Sharma SD, Katiyar SK. Honokiol, a phytochemical from the Magnolia plant, inhibits photocarcinogenesis by targeting UVB-induced inflammatory mediators and cell cycle regulators: development of topical formulation. Carcinogenesis 2010;31(11):2004–11.
Wilkey JF, Buchberger G, Saucier K, Patel SM, Eisenberg E, Nakagawa H, et al. Cyclin D1 overexpression increases susceptibility to 4-nitroquinoline-1-oxide-induced dysplasia and neoplasia in murine squamous oral epithelium. Mol Carcinog 2009;48(9):853–61.
Yang S, Yan HL, Tao QF, Yuan SX, Tang GN, Yang Y, et al. Low CADM2 expression predicts high recurrence risk of hepatocellular carcinoma patients after hepatectomy. J Cancer Res Clin Oncol 2014;140(1):109–16.
Zheng H, Ying H, Yan H, Kimmelman AC, Hiller DJ, Chen AJ, et al. p53 and Pten control neural and glioma stem/progenitor cell renewal and differentiation. Nature 2008;455(7216):1129–33.
Zhu LJ, Gazin C, Lawson ND, Pages H, Lin SM, Lapointe DS, et al. ChIPpeakAnno: a bioconductor package to annotate ChIP-seq and ChIP-chip data. BMC Bioinformatics 2010;11:237.
Zingg JM, Jones PA. Genetic and epigenetic aspects of DNA methylation on genome expression, evolution, mutation and carcinogenesis. Carcinogenesis 1997;18(5):869–82.